Langmuir
Letter
pubs.acs.org/Langmuir

Dispersing Nanoparticles in a Polymer Matrix: Are Long, Dense Polymer Tethers Really Necessary?

Grant D. Smith* and Dmitry Bedrov

Department of Materials Science and Engineering, University of Utah, Salt Lake City, Utah 84112

Received June 29, 2009. Revised Manuscript Received August 18, 2009

Dispersing nanoparticles in a polymer matrix is intrinsically challenging because of unfavorable entropic interactions between the matrix and the nanoparticle. Similar to suspensions of larger colloidal particles, it has been found that thermodynamically stable dispersions of nanoparticles can be achieved in polymer matrices when the nanoparticles are decorated with dense layers of polymer tethers whose molecular weight is comparable to or greater than that of the matrix. Utilizing molecular dynamics simulations, we demonstrate that, in contrast to larger colloidal particles, repulsive interactions between nanoparticles can be achieved with tethered polymers much shorter than the polymer matrix when relatively sparse grafting is employed.

Dispersing nanoparticles (NPs) in polymer matrices allows for the formulation of novel polymer nanocomposite (PNC) materials that combine the properties and functionality of the NP and the polymer.[1] Unfortunately, both experiment and theory reveal that dispersing nanoparticles in a polymer matrix is intrinsically difficult.[2] Theory reveals that entropic gain for the polymer associated with NP aggregation drives phase separation.[3−6] The dispersion of NPs is further complicated by energetic effects.[7] In many PNCs, particularly those employing inorganic or carbon nanoparticles, a net energetic attraction between NPs occurs as a consequence of the greater dielectric constant of the NP, resulting in net attractive London forces between the particles. These interactions, quantified by the Hamaker constant for a particular particle/matrix pair, can be strong at short range but die off quickly with increasing separation.[8] Additional attraction between NPs is possible for polar and magnetic particles.

It is clear that in many cases obtaining thermodynamically stable dispersions of NPs in polymer matrices requires the introduction of additional interactions that results in sufficient NP−NP repulsion to overcome entropic and energetic driving forces for phase separation. One approach to dispersing NPs in a polymer matrix is to modify the surface of the NPs by physically grafting (onto or from) polymers of the same composition as the polymer matrix, resulting in a polymer "brush" that will repel brushes of other particles. This polymer-grafting approach has been successfully applied to larger colloids for many years[9,10] and has been shown recently[11−14] to be effective for NPs. Much of our understanding of how grafted polymers help stabilize suspensions of NPs in polymer matrices is based on prior experience with larger colloids. For example, Borukhov and Leibler[10,15] have shown that in order to stabilize colloidal suspensions in polymer melts it is typically necessary to utilize polymer grafts whose degree of polymerization (N_g) is equal to or greater than that of the polymer matrix (N_m) as a result of the inability of the matrix to wet short brushes. This theory, developed for flat substrates and applied to explain the behavior of colloidal suspensions, has been invoked to explain the necessity of long graft chains (relative to the matrix chains) in dispersing NPs.[11−14] Furthermore, there seems to be a more is better mentality toward the use of polymer grafts in dispersing NPs (i.e., a dense brush must be more effective at dispersing particles than a sparser brush) despite the well-established fact that autophobicity (dewetting of a melt from a brush-covered substrate due to the inability of the melt to penetrate the brush) increases with increasing brush density.[10,16]

Unfortunately, the use of long grafts for NPs can pose many difficulties, not the least of which is a dramatic increase in the effective size of the NP when the radius of gyration of the grafted chain becomes comparable to or greater than the radius of the particle itself, a difficulty not encountered with larger colloidal particles. This increase in effective size reduces the achievable concentration of NPs in the composite and significantly influences the manner in which the NPs interact with other nanoscale structures such as that observed for block copolymers and immiscible blends.[14,17]

Recently, self-consistent mean-field theoretical treatments have been applied to gain understanding of the interaction of polymer-grafted spherical NPs in polymer melts[18] as well as the phase behavior of dispersions of polymer-grafted NPs in polymer matrices.[19] The former study revealed, for the specific case of $N_m = N_g$, that the effective NP−NP interaction depends strongly

(1) Winey, K. I.; Vaia, R. A. *MRS Bull.* **2007**, *32*, 314–322.
(2) Akcora, P.; Liu, H.; Kumar, S. K.; Moll, J.; Li, Y.; Benicewicz, B. C.; Schadler, L. S.; Acehan, D.; Panagiotopoulos, A. Z.; Pryamitsin, V.; Ganesan, V.; Ilavsky, J.; Thiyagarajan, P.; Colby, R. H.; Douglas, J. F. *Nat. Mater.* **2009**, *8*, 354–359.
(3) Hooper, J. B.; Schweizer, K. S. *Macromolecules* **2006**, *39*, 5133–5142.
(4) Hooper, J. B.; Schweizer, K. S. *Macromolecules* **2007**, *40*, 6998–7008.
(5) Sen, S.; Xie, Y.; Kumar, S. K.; Yang, H.; Bansal, A.; Ho, D. L.; Hall, L.; Hooper, J. B.; Schweizer, K. S. *Phys. Rev. Lett.* **2007**, *98*, 128302.
(6) Hall, L. M.; Schweizer, K. S. *J. Chem. Phys.* **2008**, *128*, 234901.
(7) Rahedi, A. J.; Douglas, J. F.; Starr, F. W. *J. Chem. Phys.* **2008**, *128*, 024902.
(8) Russel, W. B.; Saville, D. A.; Schowalter, W. R. *Colloidal Dispersions*; Cambridge University Press: New York, 1989; pp 129−158.
(9) Milner, S. T. *Science* **1991**, *251*, 905–14.
(10) Borukhov, I.; Leibler, L. *Macromolecules* **2002**, *35*, 5171–5182.
(11) Corbierre, M. K.; Cameron, N. S.; Sutton, M.; Laaziri, K.; Lennox, R. B. *Langmuir* **2005**, *21*, 6063–6072.
(12) Lan, Q.; Francis, L. F.; Bates, F. S. *J. Polym. Sci., Part B: Polym. Phys.* **2007**, *45*, 2284–2299.
(13) Wang, X.; Foltz, V. J.; Rackaitis, M.; Boehm, G. G. A. *Polymer* **2008**, *49*, 5683–5691.
(14) Xu, C.; Ohno, K.; Ladmiral, V.; Composto, R. J. *Polymer* **2008**, *49*, 3568–3577.
(15) Borukhov, I.; Leibler, L. *Phys. Rev. E* **2000**, *62*, R41–R44.
(16) Matsen, M. W.; Gardiner, J. M. *J. Chem. Phys.* **2001**, *115*, 2794–2804.
(17) Chiu, J. J.; Kim, B. J.; Kremer, E. J.; Pine, D. J. *J. Am. Chem. Soc.* **2005**, *127*, 5036–5037.
(18) Xu, J.; Qiu, F.; Zhang, H.; Yang, Y. *J. Polym. Sci., Part B: Polym. Phys.* **2006**, *44*, 2811–2820.
(19) Harton, S. E.; Kumar, S. K. *J. Polym. Sci., Part B: Polym. Phys.* **2008**, *46*, 351–358.

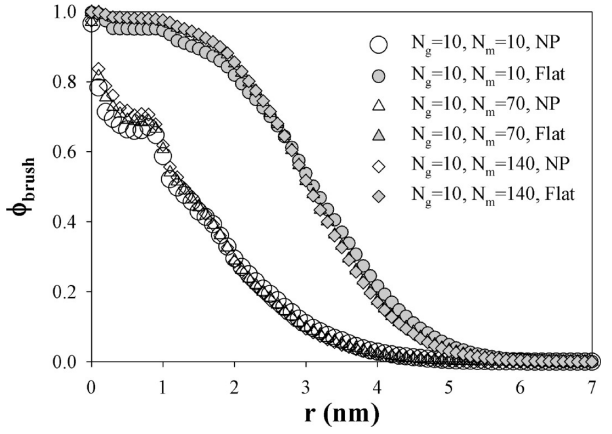

Figure 1. Brush volume fraction profiles as a function of separation from the surface as obtained for $N_g = 10$ brushes on NP and a flat surface in polymer matrices for $N_m = 10$ and 140. The $r = 0$ position corresponds to the $R_{NP} + R_{bead}$ distance from the NP center or the $2R_{bead}$ distance from the flat surface location.

on the grafting density and NP radius. For sufficiently small radius and sufficiently low grafting densities, it was predicted that effective interactions between polymer-grafted NPs will be repulsive whereas increasing grafting density and/or NP radius leads to regions of net NP−NP attraction. It was not shown in this study whether such an attraction was sufficient to overcome the entropy of mixing and lead to phase separation. In the latter study, the Scheutjens−Fleer self-consistent field model coupled with the mean-field Flory−Huggins theory was applied in order to understand better the role of surface curvature in the phase behavior of brush-covered NPs. It was found that dispersion is possible for $N_g < N_m$, unlike for larger colloids where the brush chains must typically be equal to or longer than the matrix chains. The explanation for this behavior is that the polymer brush has an increasingly large area into which it can spread as it moves away from a highly curved surface, resulting in a broader brush/matrix interface and hence relatively favorable (less repulsive) brush/matrix interactions. This effect is amplified with decreasing NP radius (i.e., the critical value of N_m/N_g; the maximum value of this ratio for which dispersion will occur increases with increasing curvature). This theoretical treatment is predicated on the strong segregation limit assumption (i.e., that a well-formed hyperbolic-tangent-shaped interface, such as shown in Figure 1 for the brushes on a flat substrate, forms between the brush and the matrix). This assumption limits the application of the theory to relatively dense brushes and results in (because of the required hyperbolic-tangent-shaped interface) unfavorable interactions between the matrix and the brush-covered NP for all situations in which the theory is applicable. Hence, in the range of applicability of the theory, dispersion is driven by the entropy of mixing alone, which, when N_m/N_g becomes sufficiently large (depending on the radius of curvature), is overwhelmed by unfavorable brush−matrix interactions.

Method

The purpose of the current study is to utilize molecular dynamics (MD) simulations to study the case of highly curved surfaces (small spherical NPs) grafted with relatively sparse brushes whose chains are short compared to the matrix chains. Given the strong influence of curvature on the interaction of polymer-grafted NPs and the phase behavior of PNCs observed in both theory and experiment, we wish to explore the possibility that interaction between the polymer-grafted NP and the polymer matrix can be favorable, or at least less unfavorable, when the polymer brush is sufficiently sparse. If so, this would indicate that a dispersion of NPs in polymer matrices may be as effectively (or even more effectively) achieved with short, sparse brushes than with longer, dense brushes. Details of the molecular simulation model are given in the Supporting Information. The coarse-grained bead−spring model employed in our simulations has been mapped to "real" spatial units by matching the contour length and radius of gyration of the polymer chains with that of poly(methyl methacrylate) (PMMA), yielding a fundamental length scale (polymer bead diameter) of 1 nm. We report all quantities in terms of real spatial units based upon this mapping. The coarse-grained MD simulations were performed on a single polymer-grafted NP with a diameter of 5 nm as well as for a pair of these NPs in melts of the same (coarse-grained PMMA) polymer.

Results

Brush Volume Fraction Profile. For the single NP, the brush volume fraction profile, given as the fraction of polymer units belonging to grafted chains (as opposed to the matrix) as a function of separation from the particle surface, was determined for grafted chains of 10 beads ($N_g = 10$, corresponding to a PMMA molecular weight of 2.7 kDa) in polymer matrices with lengths of $N_m = 10$, 70, and 140 beads, corresponding to PMMA molecular weights of 2.7, 13, and 37 kDa, respectively. A grafting density of $s = 0.4$ chains/nm^2 (30 chains) was investigated. The dimensionless relative grafting density is given as

$$s^* = \frac{\frac{N}{4\pi R_p^2}}{\frac{1}{\pi\langle R_g^2\rangle}} = \frac{N\langle R_g^2\rangle}{4R_p^2} \quad (1)$$

where N is the number of grafted chains (30), R_p is the NP radius (2.5 nm) and $\langle R_g^2\rangle$ is the mean-square radius of gyration of the grafted chains. Simulation studies of melts of $N = 10$ chains yielded a mean-square radius of gyration of $\langle R_g^2\rangle = 2.2$ nm^2. Hence, a grafting density of $s = 0.4$ chains/nm^2 corresponds to $s^* = 2.64$, indicating a dense brush.

We also investigated the brush profile for a flat substrate at the same graft length, grafting density, and matrix length. A comparison of the brush volume fraction profiles for the 5 nm NP and the flat substrate is shown in Figure 1. Clearly noticeable is the dramatic, qualitative difference in the profiles for the different substrates. For the flat substrate, the profiles exhibit the expected hyberbolic-tangent shape that becomes narrower, and hence more repulsive or dewetting in character, with increasing N_m/N_g. A clear "dry" brush region, a region near the substrate into which the polymer matrix does not penetrate, can be observed. For the highly curved NP, in contrast, the polymer matrix penetrates to the particle surface, even for $N_m/N_g \gg 1$. No dry brush region is observed, and the interface subsequently does not exhibit a hyperbolic tangent profile. The brush profile for the NP is encouraging in that it is indicative of a matrix−brush interaction that is much less unfavorable than for the equivalent flat substrate.

Effective Interaction between Nanoparticles. For simulations involving two polymer-grafted NPs, the free energy as a function of NP−NP center-of-mass separation (the potential of mean force, or POMF) was determined as described in the Supporting Information. For this study, the NPs have the same grafting chain length ($N_g = 10$) and grafting density of $s = 0.4$ chains/nm^2 ($s^* = 2.64$) in matrices of length $N_m = 10$, 70, and 140. Snapshots from two NP simulations with $N_m = 10$ and $N_m = 140$ are shown Figure 2. Figure 3 shows the POMF as a function of the NP center-of-mass separation for the three matrix lengths. At large separation, no interaction between the polymer-grafted nanoparticles is observed, and the free energy is independent

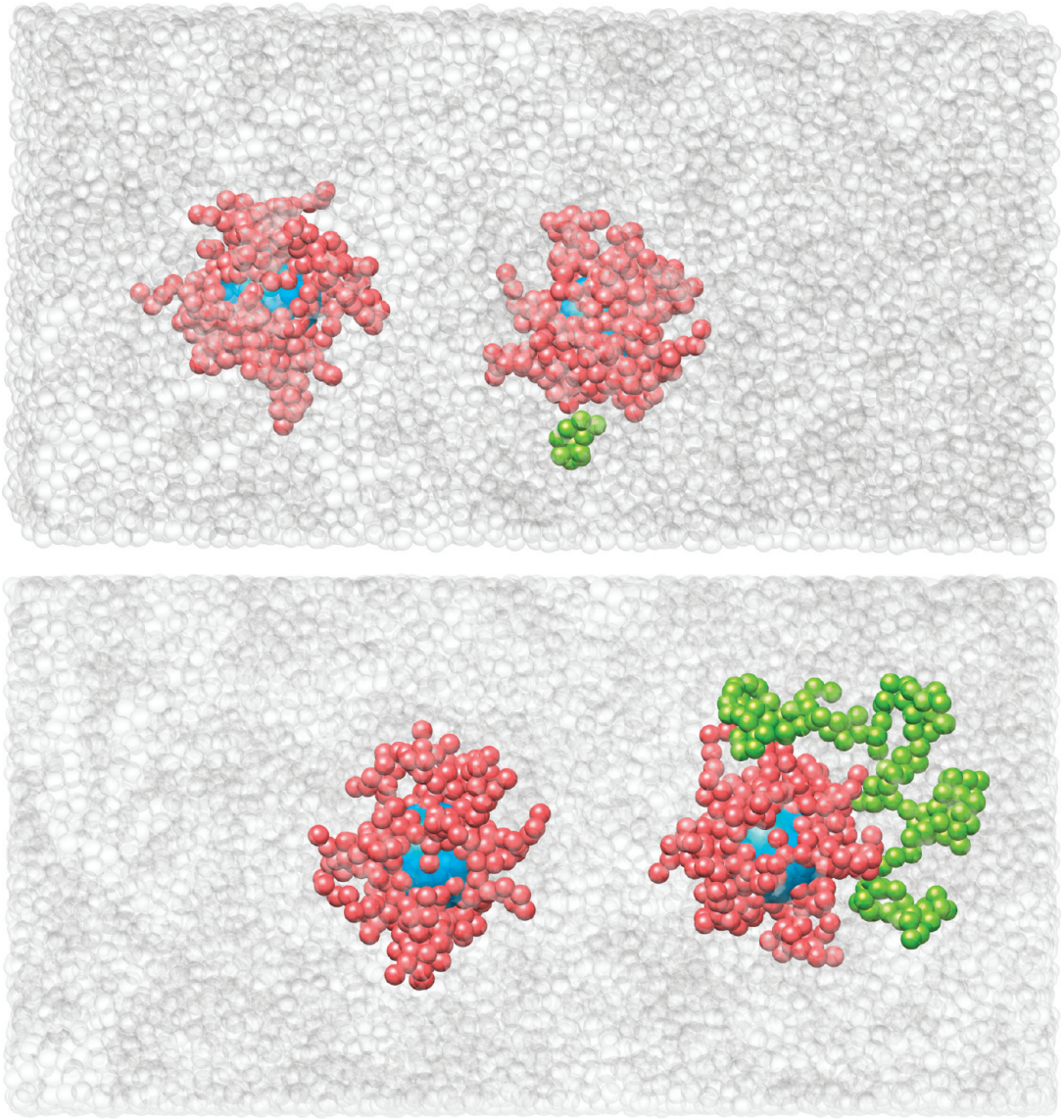

Figure 2. Snapshots of two polymer-modified NPs in polymer matrices with $N_m = 10$ (top) and 140 (bottom). The size of all matrix beads, with the exception of one chain, is reduced for visual clarity. One randomly selected chain in the matrix is shown at full size (green beads).

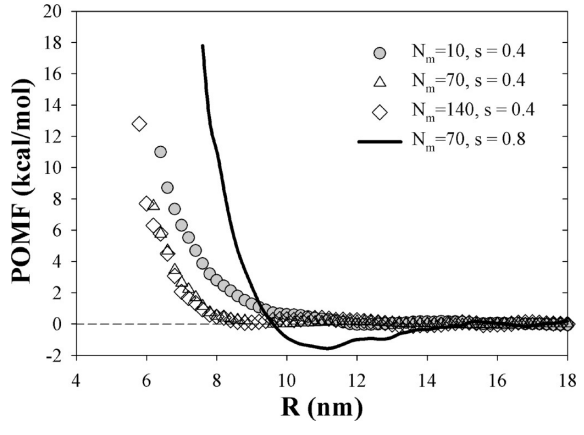

Figure 3. POMF between two NPs modified with $N_g = 10$, with a grafting density of $s = 0.4$ chains/nm^2 as a function of the separation of NP centers (R) in various matrices. The POMF does not include any direct NP−NP interaction.

of separation within computational uncertainties. For the short matrix chains ($N_m = 10$), a net repulsive interaction between nanoparticles is observed for separations of <11 nm. At this separation, the surface−surface separation between particles is 6 nm, which corresponds to a distance where we would expect two brushes to start to overlap significantly (Figure 1) and hence exert repulsive forces on each other. Figure 3 reveals that with increasing matrix chain length the range and magnitude of the repulsive interaction decrease. This is not due to any significant difference in the brush density profile (Figure 1) or hence to differences in the brush−brush repulsion. Rather, we believe that it indicates that the interaction between the brush and the matrix becomes less favorable with increasing matrix molecular weight, as expected. However, we note that even for $N_m/N_g = 14$ the net interaction between the polymer-grafted NPs remains either negligible (intermediate and large separation) or repulsive (small separations), indicating that even at this ratio (i.e., for very long matrix chains compared with the graft chains) we would anticipate NP dispersion. Moreover, Figure 3 shows that POMF for $N_m = 70$ and 140 differ little, indicating the potential saturation of unfavorable brush−matrix interactions with increasing matrix molecular weight, hence allowing us to suggest that further increases in N_m would not significantly change the POMF.

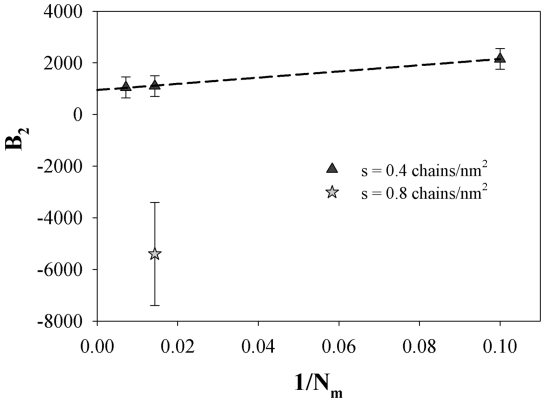

Figure 4. Second virial coefficient B_2 for NP modified with N_g = 10 grafted chains as a function of the inverse chain length of the matrix, N_m, as obtained using eq 1 and POMF obtained from coarse-grained MD simulations (Figure 3).

Second Virial Coefficient and Comparison with Experiment. Using the (effective) interparticle potential given by the POMF (Figure 3), the second virial coefficient B_2 is given as[20]

$$B_2 = 2\pi \int_0^\infty \mathrm{d}r\, [1 - \exp(-\mathrm{POMF}(r)/k_\mathrm{B}T)] \qquad (2)$$

For positive values of B_2, we anticipate particle dispersion, whereas sufficiently large negative values are expected to result in phase separation.[20] Values of B_2 for the potentials shown in Figure 3 with a grafting density of s = 0.4 chains/nm^2 (s^* = 2.64) are shown in Figure 4. The positive values of B_2, and hence anticipated NP dispersion, are consistent with the fact that the effective interparticle potential is positive at all separations. Whereas B_2 becomes less positive with increasing matrix molecular weight, it appears from Figure 4 that the 5 nm NPs with N_g = 10 should disperse in any molecular-weight matrix.

Influence of Polymer Grafting Density. Our choices of NP diameter, graft chain length, and matrix chain lengths for this study were guided by a recently published experimental study of the dispersion of PMMA-grafted ferrite nanoparticles[21] in a PMMA matrix.[14] According to this study, the dispersion of 5−7 nm ferrite NPs in a 37 kDa matrix (equivalent to N_m = 140) does not occur for a brush length of 2.7 kDa (equivalent to N_g = 10). Instead, strong aggregation is observed, in stark contrast to our predictions. Experiments reveal that a much longer brush, between 13 kDa (aggregation observed) and 37 kDa (dispersion observed), is required to disperse the NPs.

It has been estimated that Hamaker interactions and magnetic interactions are insufficient alone to account for the observed aggregation behavior for the short and intermediate-length brushes for the PMMA/ferrite NP composite.[14] Hence, autophobic interactions (unfavorable interactions between the brush and the matrix) appear to be the driving aggregation for the PMMA-grafted ferrite, despite the fact that our MD simulations predict net repulsive interactions at all separations for the equivalent coarse-grained system (Figure 3) and a corresponding positive value for B_2 (Figure 4). We believe that this discrepancy is due to the difference in grafting density between our simulated polymer-grafted NPs and those examined experimentally. Whereas our grafting density is about 0.4 chains/nm^2, the experimental grafting density is significantly higher, around 0.7 to 0.8 chains/nm^2. To validate this supposition, we have carried out additional simulations of a single NP and an NP pair at a higher grafting density of 0.8 chains/nm^2 (N = 60 chains, s^* = 5.28) with N_g = 10 in a matrix of N_m = 70. A snapshot of the NPs (N_g = 10, N_m = 70) for the two grafting densities (0.4 and 0.8 chains/nm^2) is shown in Figure 5, revealing that whereas the NP surface is exposed for the lower grafting density, allowing the matrix to penetrate to the NP surface, the NP surface does not appear to be exposed to the matrix at the higher grafting density. This conclusion is supported by the brush volume fraction profiles shown in Figure 6, where it can be seen that there is a negligible matrix density near the NP surface at the higher grafting density. In fact, the brush volume fraction profile at this higher density more closely resembles that for the flat substrate at the lower grafting density, including a hyberbolic tangent interfacial profile and a dry region near the particle surface, than it does the brush profile for the NP at the lower grafting density.

In Figure 3, the POMF between two NPs with N_g = 10, N_m = 70, and s = 0.8 chains/nm^2 (s^* = 5.28) is compared with POMFs obtained for the lower (0.4 chains/nm^2) grafting density. Whereas for latter there is no regime of net attraction between the nanoparticles as discussed above, at the higher grafting density attraction is observed. We note that these results are consistent with the theory of Fredrickson et al.[22] for blends of star polymers and chemically identical linear polymers, where decreasing miscibility is predicted for stars with an increasing number of arms. The net NP−NP attraction observed in our simulations is likely the result of increased autophobic interactions between the denser brush and the matrix at the higher grafting density that are not fully offset by the greater range of brush−brush repulsion expected for the more extended brush at the higher grafting density (Figure 6). Utilizing eq 2, we have determined B_2 for the N_g = 10, N_m = 70, s = 0.8 chains/nm^2 system, which is shown in Figure 4. Increasing the grafting density results in a large, negative value of B_2, sufficiently negative that phase separation of the NPs is predicted according to the extended corresponding-states approach of Noro and Frenkel.[20] Hence, it appears that a likely source of the aggregation observed in the ferrite−PMMA system for the short brush is autophobicity engendered by the high density of the polymer brush.

Influence of Polymer Grafting Length. Although we predict the dispersion of the 5 nm NPs with grafted chains of length N_g = 10 and $N_m \leq 140$ (and likely for even longer matrix chains) at a grafting density of 0.4 chains/nm^2, the NPs with this short brush are able to approach quite closely (Figure 3) before brush−brush repulsion becomes dominant and the repulsive force becomes significant. For systems with larger Hamaker and/or magnetic interactions or for larger NPs where the range of these interactions is correspondingly greater, this short brush may not be sufficient to promote dispersion. Increasing the density of the grafted polymer is *not* the solution to this problem, as revealed by the discussion above. Rather, we recommend the use of longer grafted chains at a similar grafting density. Because Hamaker and magnetic interactions die off rapidly with separation, it is necessary to increase the separation at which significant brush−brush repulsion between NPs is observed by only a few nanometers in order for these effects to become negligible. The brush volume fraction profile for the 5 nm NP is shown in Figure 6 for a longer graft (N_g = 40), with N_m = 140 and s = 0.4 chains/nm^2, corresponding to s^* = 11.6 (eq 1). Importantly, the longer graft chains result in a more extended brush, thereby increasing the

(20) Noro, M. G.; Frenkel, D. *J. Chem. Phys.* **2000**, *113*, 2941–2944.
(21) Ohno, K.; Morinaga, T.; Koh, K.; Tsujii, Y.; Fukuda, T. *Macromolecules* **2005**, *38*, 2137–2142.
(22) Fredrickson, G. H.; Liu, A.; Bates, F. S. *Macromolecules* **1994**, *27*, 2503–2511.

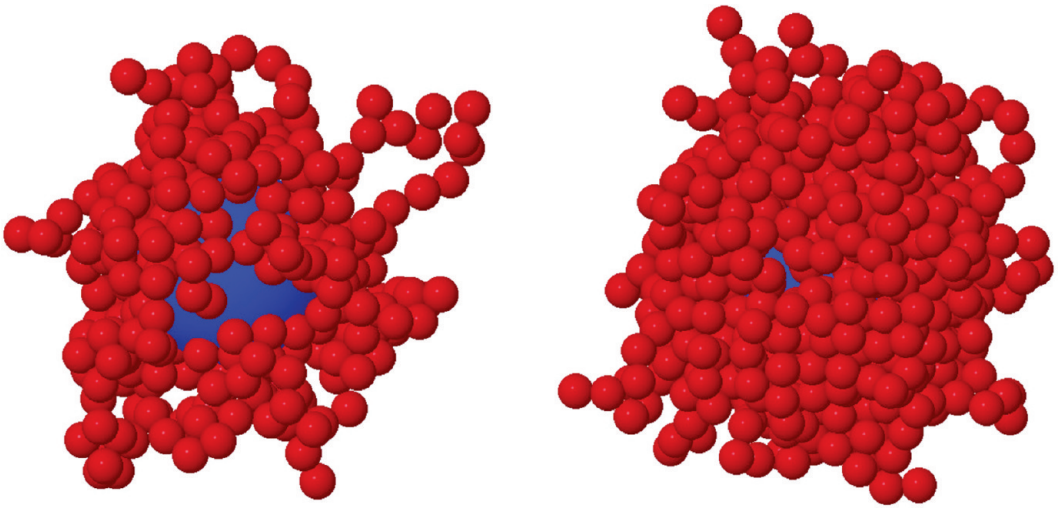

Figure 5. Snapshot of the single particles at low (left) and high (right) grafting densities in the $N_m = 70$ matrix. Matrix chains are not shown.

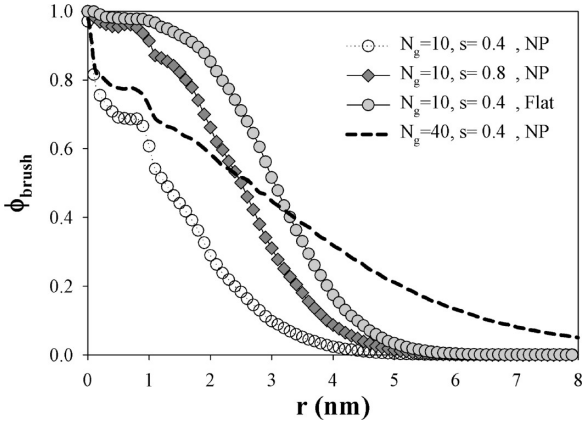

Figure 6. Brush volume fraction profiles as a function of separation from the surface as obtained for selected (see the text) NP and flat surface systems in polymer matrix $N_m = 70$.

expected range of brush−brush repulsion while at the same time allowing the matrix to penetrate to the particle surface in a manner similar to that observed for the shorter chains. We therefore anticipate only net repulsive NP−NP interactions for this brush that become significantly repulsive at greater separation than for the short brush.

Surface Curvature and Relative Grafting Density. Finally, we wish to explore briefly the relationship between surface curvature and the relative grafting density. For the three brushes studied here, namely, $N_g = 10$ and $s = 0.4$ chains/nm^2, $N_g = 10$ and $s = 0.8$ chains/nm^2, and $N_g = 40$ and $s = 0.4$ chains/nm^2, the dimensionless effective grafting densities (from eq 1) are $s^* = 2.64$, 5.28, and 11.6, respectively. In all cases, the grafting density corresponds to a dense brush. However, only in the second case (i.e., the case with the higher number of grafted chains) does the brush volume fraction profile (Figure 6) exhibit behavior consistent with a dense brush. As discussed above, the curvature of the NP surface allows the polymer brush to spread out as it moves away from the surface. We can utilize eq 1 to estimate at what distance d from the NP surface the brush will transition from a dense brush to a "mushroom":

$$d = \left(\frac{N\langle R_g^2\rangle}{4}\right)^{1/4} - R_p \qquad (3)$$

Equation 3 was derived by rearranging eq 1 with $s^* = 1$ and replacing R_p with $R_p + d$. For $N_g = 10$, we obtain $d = 1.6$ and 3.2 nm for the low and high grafting densities, respectively. We find that 58% of the grafted polymer beads lie farther than 1.6 nm from the NP surface for the low-density brush, indicating that the majority of units experience a mushroom environment due to surface curvature. In contrast, only 23% of the grafted polymer beads lie farther than 3.2 nm from the surface for the high grafting density, indicating that in this case the majority of beads experience a dense brush environment. The brush of longer chains at the low grafting density, which has a large value of s^* because of the increased radius of gyration of the longer chains, is intermediate between these two cases. Whereas this simplified picture has its limitations, it serves to illustrate the importance of surface curvature and the inapplicability of s^* as a scaling variable.

Summary. Dense polymer brushes can lead to a dispersion of NPs polymer matrixes when the length of the grafted chains is comparable to that of the matrix. At lower grafting densities, where matrix chains are able to penetrate to the surface of the particle as a result of strong curvature effects, the matrix−brush interaction is much less unfavorable and the net effect of brush−brush repulsion (leading to dispersion) and brush matrix repulsion (leading to aggregation) is dominated by the former even for matrices that are significantly longer than the grafted chain. The grafted chains must be sufficiently long, however, to ensure that strong repulsion between the nanoparticles sets in at a sufficiently large distance such that direct attractive interactions between the nanoparticles, such as Hamaker interactions and magnetic interactions, are weak. An intriguing solution to this problem may be the use of mixed polymer brushes. A relatively dense, very short brush is applied to prevent direct NP−NP contact. These particles will aggregate in long matrixes as a result of autophobic interactions with the matrix. This can be prevented by applying a somewhat larger, but relatively sparse, brush that results in brush−brush repulsion but is sparse enough to have minimum autophobic effects.

Acknowledgment. We gratefully acknowledge the financial support of this work by the National Science Foundation through the Liquid Crystal MRSEC (University of Colorado, DMR-0213918). We also thank Professor Russell Composto for valuable discussions.

Supporting Information Available: Model and single-nanoparticle, surface, and two-nanoparticle simulations. This material is available free of charge via the Internet at http://pubs.acs.org.